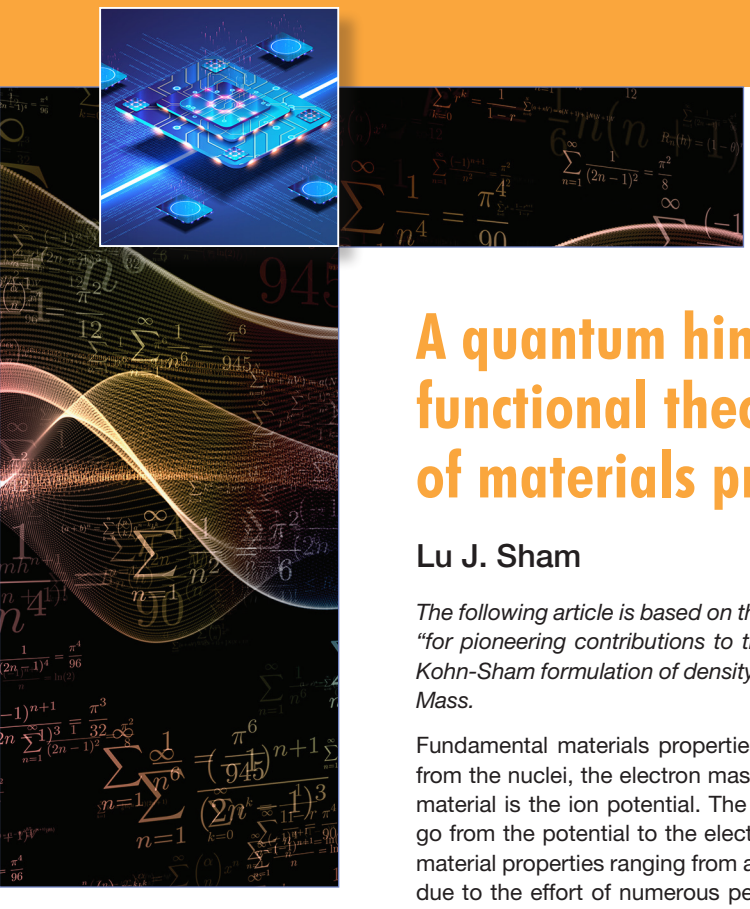

A quantum hindsight on density functional theory for computation of materials properties

Lu J. Sham

The following article is based on the Materials Theory Award presentation given by Lu J. Sham "for pioneering contributions to the quantum theory of molecules and solids, especially the Kohn-Sham formulation of density functional theory," at the 2019 MRS Fall Meeting in Boston, Mass.

Fundamental materials properties are determined by electrons under the potential energy from the nuclei, the electron mass, and their mutual repulsion. The variable from material to material is the ion potential. The logical procedure of computing electronic properties is to go from the potential to the electron distribution. This enables practical computation of the material properties ranging from atoms and molecules to solids. This method has blossomed due to the effort of numerous people. The concept is analogous to changing prediction of human population distribution from the landscape of hills and dales to determination of the landscape from a population distribution. In atomic systems, quantum quirkiness allows this switch, but dictates that it is only one slice in the tomography of the quantum state. The author shares his experience in the development from this slice, but hews close to the powerful concept of switching the landscape with the population.

Introduction

For 55 years, density functional theory (DFT), founded by the fundamental Hohenberg–Kohn (HK) theorem[1] and the practical Kohn–Sham (KS) equation,[2] has flourished, due to advances in computation methods and applications to materials properties. Advances in computation have been fueled by tremendous innovations in formulating the exchange and correlation functional potentials in the KS equation empirically for large classes of systems and open computation program apps in the free spirit of the internet in its pioneering days. Further development of the theory and applications does not seem to be flattening.

In the early 1960s, single-electron-band structure computations had become reliable[3] and the interacting electron gas treated by field-theoretic methods went beyond the Hartree–Fock approximation to include correlation effects by, for example, the random phase approximation[4] or the ring diagrams.[5] There was the dichotomy of the former looking for a reliable effective potential for the single electron and the latter being limited to the jellium (a uniform background of positive charges) extended somewhat to simple metals. DFT then built a bridge to bring the exchange and correlation effects to the band calculation.

The DFT field has become too vast to review in a single article. I will use a thread of what I have been involved in to examine the field from a quantum perspective. This spans from the old quantum criterion of state coherence to the quantum information era requirement of entanglement. The former drives, for example, density oscillations due to an impurity in a metal or the electron density shell structure in atoms, while the latter is concerned with what phenomena entanglement can drive. We examine how DFT elucidates such quantum phenomena in various systems.

Hohenberg–Kohn theorem and the state topography

The HK theorem[1] forms the foundation of DFT. It allows the ground-state energy of a many-electron state to be determined by the knowledge of the electron-density distribution as a function of electron position instead of its potential. The use of the variational principle of the ground-state energy as a function of the density allows it to be determined for a given single-electron potential. This work reaches the pinnacle of the improvement of the Thomas–Fermi theory. The important point is the introduction of the Legendre transformation from the potential $v(r)$ to the density $n(r)$. The

Lu J. Sham, University of California, San Diego, USA; ljssst@physics.ucsd.edu
doi:10.1557/mrs.2020.192

transformation has the convenience for computation that can be extended to other duality pairs. An example is next presented.

The complete characterization of a quantum state in an experiment requires tomography (i.e., a series of measurements of non-commutative observables).[6,7] From the quantum viewpoint, the dependence on the density is akin to a slice of the tomography. The variational equation of the ground-state energy in terms of the density distribution alone cannot recover the loss of phase information in the electron-density distribution. Even in the case where the electron–electron interaction is neglected, attempts with gradient expansion cannot remedy this phase loss, as the history of numerous attempts to improve the Thomas–Fermi equations by adding higher-order gradient terms to find the shell structure of the electron in an atom had shown.

The problem does not lie in the slowly varying approximation. The quantum effect of density oscillations as a function of position has been demonstrated by computation using the slowly varying WKBJ approximation of the wave function of the Schrödinger equation.[8] The quantum effect is driven by the confinement effect to produce a standing wave from the turning point (where the potential equals the electron energy). Interestingly, the wave behavior is determined mostly by the energy states close to the highest occupied states. There, the connection between the oscillatory functions and the decaying functions are not determined by sinusoidal and the exponential waves, but more accurately, by the corresponding oscillating and decaying Bessel function solutions of the linear portion of the potential bracketing the turning point.[9] The method of finding oscillations also applies to nuclear matter density.[10] This is also the cause of the Friedel oscillations[11] due to an impurity potential in a metal being the state of energy just below the Fermi level.

Quantum phase transition via DFT

The quantum phase transition (QPT)[12,13] is a critical change in the ground-state properties of a material system. It can be observed at very low temperatures. Consider a material's Hamiltonian,

$$\hat{H} = \hat{H}_0 + \hat{H}_{\text{ext}} = \sum \lambda_l \hat{A}_l, \tag{1}$$

where l is the lattice site and $\hat{A}$ is an observable driven by the external field parameter λ_l. QPT is usually characterized by the change of the ground-state energy as a nonanalytic point on varying the field parameters (i.e., external forces), in the Hamiltonian, (e.g., a first-order QPT at a finite discontinuity and a second-order one at a discontinuous derivative).

An extension of the Hohenberg–Kohn theorem is to make a Legendre transformation of the ground-state energy as a function of the field parameters λ_l to its conjugate pairs, viz. the set of ground-state expectation values $a_l = \langle \hat{A} \rangle$. If we regard the set of $\{a_l\}$ as the results of simultaneous quantum measurements of the observables $\hat{A}$, the set of the observables has to be commutative. The rule permits a certain amount of latitude, such as having noncommutative pairs, the spin components $\hat{S}_l^x \hat{S}_l^y$, or two-site operators $\{\hat{A}_l \hat{A}_{l+c}\}$ for all l sites and a constant, c. A simple connection between the λ_l representation and the $\{a_l\}$ representation is by the Hellmann–Feynman theorem for the ground-state energy E,

$$\frac{\partial E}{\partial \lambda_l} = \left\langle \frac{\partial \hat{H}}{\partial \lambda_l} \right\rangle = \left\langle \hat{A} \right\rangle = a_j, \tag{2}$$

where $\langle \ldots \rangle$ denotes a ground-state expectation value.

One method to detect the QPT point is to use a measure of the quantum entanglement of the material system. The entanglement between two qubits, for example, two states of each of a pair of spins, is the correlation between two spins at any distance apart. Consider the singlet or one triplet state of the two spins,

$$|\psi\mp\rangle = |\uparrow\rangle_1 |\downarrow\rangle_2 \mp |\downarrow\rangle_1 |\uparrow\rangle_2. \tag{3}$$

The two spins are entangled. If the first spin is measured to be up, then the second spin has to be down and vice versa. This can happen even if one spin is half a world apart from the other, described famously by Einstein as "spooky action at a distance." In a many-body system, the entanglement may be considered to be bipartite (between two parts) or multipartite (between multiple parts). The bipartite can be even just one qubit with the rest of the system. The quantitative entanglement measure may be the entropy or simplified to just an appropriate log function as a function of the field parameters $\{\lambda_l\}$,

$$L_l^{(2)} = 1 - \nabla_l E \bullet \nabla_l E. \tag{4}$$

The entanglement measure with the field parameter variation may be used to detect QPT.[14] We showed[12] that the use of the conjugate partner $\{a_l\}$ in the Legendre transformation was not only possible, but could cover the whole range, rather than being confined to the critical region near the phase transition point as was done with field parameters. Equation 4 was used to express the entanglement measure.

A model with existing theory and experiment is the transverse-field Ising model in which $\hat{H}_0$ is the Ising model of antiparallel spin pairs in one direction and $\hat{H}_l$ has the magnetic field normal to that direction. The density functional numerical computation led to a clear indication of the critical point at the linear model with 1000 sites. The use of other entanglement measures also confirmed the QPT point.

The KS equation

The missing observable of importance in the density functional variational equation is the momentum that does not commute with the position. The KS equation[2] can thus be seen as an attempt to restore this quantum feature while

https://doi.org/10.1557/mrs.2020.192 Published online by Cambridge University Press

keeping the density functional nature of the observables in the Hamiltonian that commute with the density observable. The ground-state energy, E, was divided into two functional components,

$$E = T_s[n] + V[n], \tag{5}$$

where $T_s[n]$ is the kinetic energy functional of the density n borrowed from the single-particle case, and $V[n]$ includes both the single-particle potential and all of the interaction effects, usually divided into the electrostatic form of the Coulomb interaction energy and the exchange-correlation term that includes the kinetic energy contribution,

$$V[n] = \int d^3r v(\mathrm{r}) n(\mathrm{r}) + \int d^3r \int d^3r' \frac{n(\mathrm{r}) n(\mathrm{r}')}{2|\mathrm{r}-\mathrm{r}'|} + E_{xc}[n(\mathrm{r})]. \tag{6}$$

This division follows the practice of the homogeneous electron gas case and has the energy functional form of a single electron with the Schrödinger equation,

$$\left[-\frac{h^2}{2m}\nabla^2 + v_{\mathrm{eff}}(\mathrm{r})\right]\psi_j(\mathrm{r}) = \varepsilon_j \psi_j(\mathrm{r}), \tag{7}$$

where the effective potential is derived from the functional derivative of $V[n]$,

$$(\mathrm{r}) = v(\mathrm{r}) + e^2 \int d^3r' \frac{n(\mathrm{r}')}{|\mathrm{r}-\mathrm{r}'|} + v_{xc}[n(\mathrm{r})], \tag{8}$$

$$v_{xc}[n(\mathrm{r})] = \frac{\delta E_{xc}[n(\mathrm{r})]}{\delta n(\mathrm{r})}, \tag{9}$$

and the density is given by the orbitals,

$$n(\mathbf{r}) = \sum_j^N |\psi_j(\mathbf{r})|^2. \tag{10}$$

The previously discussed process of going from the classical variational equation to the quantum Schrödinger equation is clearly not a derivation, rather, it depends on the reverse procedure from a system of independent electrons to its variational density functional equation. From the viewpoint of the tomography analogy, Equation 5 is a convenient split-up for the quantum leap. The process of deriving from the many-electron theory the exchange-correlation potential $v_{xc}[n(\mathbf{r})]$ for a given $v(\mathbf{r})$ is then possible (see next section).

The KS paper[2] provided the local density approximation (LDA) for $v_{xc}[n(\mathbf{r})]$ by assuming that the functional $E_{xc}[n(\mathbf{r})]$ is given by the homogeneous gas expression with the density dependent on the position $\mathbf{r}$. The LDA, including the spin part, has been used for quite a few solid-state systems, particularly simple metals and surfaces, but has been found to not work well for molecules in particular. This shortcoming spurred the innovation of numerous exchange-correlation functionals better suited to being used for molecules.[15]

The field-theoretic approach

The tool used to find the single-electron property under the influence of both the single-electron potential $v(\mathbf{r})$ and the interaction with other electrons is the Green's function in energy, $G(\mathbf{r},\mathbf{r}';E)$.[16] Green's function is governed by the Dyson equation,

$$\left[-E - \nabla^2 + v_e(\mathbf{r})\right] G(\mathbf{r},\mathbf{r}';E) + \int d^3\mathbf{r}'' \Sigma(\mathbf{r},\mathbf{r}'') G(\mathrm{r}'',\mathrm{r}';E) = -\delta(\mathbf{r},\mathbf{r}'), \tag{11}$$

where v_e is an "effective potential" for this equation, $\Sigma(\mathbf{r},\mathbf{r}')$ is the self-energy or mass operator. The choice of v_e is flexible. For example: we could take v_e to be (1) zero, (2) v the ion potential, or (3) v_{eff} in Equation 8. The self-energy contains the interaction between two electrons and compensates for any single-particle potential taken by v_e.

The field-theoretic approach is a perturbative one in which Green's function is expanded as a power series in the self-energy as the perturbation connected by the unperturbed Green's function, $G_0(\mathbf{r},\mathbf{r}';E)$, governed only by v_e. A pole of the full Green function in the complex energy plane is taken to be a quasiparticle with the real part of its complex E value as the quasiparticle energy and the imaginary part its decay rate. Near the Fermi level of a metal, the decay rate is long and the quasiparticles behave like independent particles.

The quasiparticle energy in the inhomogeneous electron gas

The single-electron energies from the KS equation are not truly those of the quasiparticles. To find an approximation for the quasiparticle energy,[16] the same philosophy of LDA for the ground state is applied to the self-energy. The self-energy is split into the one-particle potential, including the electrostatic potential (the Hartree potential) v_{ht} and the exchange and correlation part of the homogeneous electron gas $\mathbf{M}_h$.

$$\Sigma(\mathbf{r},\mathbf{r}') = v_{ht}(\mathrm{r})\delta(\mathbf{r}-\mathbf{r}') + \mathrm{M}_h\left(\mathbf{r}-\mathbf{r}';E - v_{ht}\left(\frac{\mathrm{r}+\mathrm{r}^2}{2}\right)\right). \tag{12}$$

For the two-point function of the self-energy at $\mathbf{r}$ and $\mathbf{r}'$, we use the mean $1/2(\mathrm{r}+\mathrm{r}')$ as the location of the neighborhood and the half distance between the two points as the radius. The energy zero of the local electron gas is the local Hartree potential. The homogeneous electron gas approximation is justified by the argument that, for the homogeneous electron gas, the dominant part of $\mathbf{M}_h$ is in the neighborhood of a small diameter of $|\mathbf{r}-\mathbf{r}'| \sim 1/k_F$, the inverse of the local Fermi vector. We follow the Wigner distribution assignment of the neighborhood[17] for a similar cause. In the Wigner case, the classical state probability in thermal equilibrium was a partition function of the particle momentum and position. For the quantum system, he replaced the state probability with the noncommutative operators of position and momentum and constructed

https://doi.org/10.1557/mrs.2020.192 Published online by Cambridge University Press

the famous Wigner probability function in terms of the sum and difference of two points in position.

A derivation of the density functional exchange and correlation potential

Numerous authors have written that the exchange-correlation functional $E_{xc}[n]$ is "unknown." In fact, a general expression may be derived from the many body theory for $E_{xc}[n]$.[18] A coefficient λ is attached to the interaction term in the Hamiltonian,

$$\hat{H}(\lambda) = \hat{H}_0 + \lambda \hat{H}_1, \tag{13}$$

so that as λ is varied from 0 to 1, the total Hamiltonian will move from the independent particle one to the one with the full electron interaction. The noninteracting particle part $\hat{H}_0$ is designed to treating the full KS equation for the independent electrons under the influence of the total effective potential $v_{\text{eff}}(\mathbf{r})$ in Equation 8. The interaction part $\hat{H}_1$ includes the usual interaction between two electrons minus the effective single-particle potential term driven by $v_{\text{eff}}(\mathbf{r}) - v(\mathbf{r})$ so that the interaction effect in $\hat{H}_0$ is not double counted.

Following the field-theoretic procedure of Luttinger and Ward,[19] the ground-state energy is given by the coupling constant integral,

$$E = E_0 + \int_0^1 \frac{d\lambda}{\lambda} \langle \lambda \rangle_\lambda, \tag{14}$$

where E_0 is the ground-state energy of $\hat{H}_0$ and the angular brackets denote the exact ground-state expectation. From the infinite perturbation series in terms of Green's function in the Feynman diagrams,[20] the integral leads to,

$$E_{xc}[n] = i\text{Tr}\left[\ln(1 - \Sigma G_0) + \Sigma G\right] + Y_{xc}, \tag{15}$$

where Tr denote the trace and Y_{xc} is the exchange-correlation part of the energy diagrams of the dressed Green function, G. The formula for the exchange and correlation $v_{xc}[n]$ then follows. Its validity depends on the validity of the perturbation series. The simplicity of the LDA is gone, but the complexity is necessary in a number of cases. An example is shown next.

The bandgap problem

The band structure computations solving the KS equation with the local density approximation[2] were widely applied to the electron-band structures of materials. By the early 1980s, it was found that the computed semiconductor bandgaps were quite generally about 2/3 of the experimental values. Perdew and Levy[21] and Sham and Schlüter[22] pointed out the discontinuity in the DFT, which was absent in LDA based on the metallic electron gas. The Sham–Schlüter argument was based on the Green's function formulation in Equation 15 and was able to show a model result[23] and, moreover, detailed computations. In collaboration with Lannoo, we studied the correction to the bandgap via a model study.[24] With Godby, we computed the band structures of Group IV and III–V semiconductors beyond LDA, as detailed next.

The energy gap of an insulator by Green's function method

First, we precisely define the bandgap E_g.

$$E_g = \varepsilon_c - \varepsilon_v = \left[E_{N+1} - E_N\right] - \left[E_N - E_{N-1}\right], \tag{16}$$

where E_M is the lowest state energy of M electrons. The gap is then divided into two parts,

$$E_g = \varepsilon_g + \Delta_{xc}, \tag{17}$$

where ε_g is the bandgap defined by the KS eigenvalues and Δ_{xc}, the gap addition,

$$\Delta_{xc} = \int \left[\frac{\delta E_{xc}[n]}{\delta n_+} - \frac{\delta E_{xc}[n]}{\delta n_-}\right] |\psi_{N+1}(N)|^2, \tag{18}$$

where the position $\mathbf{r}$ in the integral is understood. The suffixes + and – denote the functional derivatives above and below N respectively and $\psi_j(N)$ is the j-th KS orbital of the N particle state. The gap addition is solved by the Green's function method.

Model study

For a two-band plane-wave model in one dimension,[23] the Hartree–Fock approximation, including only the exchange term, demonstrates a gap discrepancy comparable to the KS gap. When the correlation is added in the random phase approximation, which yields a dynamically screened interaction between two electrons, the bandgap due to discontinuity Δ_{xc} is shown.[24]

Computation of band structures of common semiconductors

Computations of the electron-band structures of semiconductors by Godby, Schlüter, and Sham used the Green's function method described above. The dielectric screening and the self-energy were approximated by the random phase approximation.

For Si,[25] v_{xc} beyond LDA was calculated. The gap computed with the Green's function method is in good agreement with experiments. If the LDA gap is raised by the calculated discontinuity Δ_{xc}, then the energies at symmetry points of the Brillouin zone are quite similar to the LDA ones. This feature is not shared by the results for the III–V compounds.

For GaAs and AlAs,[26] the quasiparticle energies computed at the symmetry points are in general in good agreement with experiments. One exception is the L point conduction minimum of AlAs. The paper suggested,[26] with some optical data support, the discrepancy was due to the extrapolation of the experimental data from a range of alloys of $Al_xGa_{1-x}As$ to pure AlAs.

For the series of semiconductors, ranging from small to large measured bandgaps of Si, GaAs, AlAs, diamond,[27] we examined the trends in the self-energies, the exchange-correlation

https://doi.org/10.1557/mrs.2020.192 Published online by Cambridge University Press

potentials v_{xc}, and the gap discontinuities Δ_{xc}. The self-energies are in good agreement with the measured quasiparticle energies. Thus, the KS eigenvalues from the self-energy computation are distinct from the LDA values.

The self-energy $\Sigma(\mathbf{r},\mathbf{r}';E)$ can be fit to the formula,

$$\Sigma(\mathbf{r},\mathbf{r}';E) \approx \frac{1}{2}\left[f(\mathbf{r})+f(\mathbf{r}')\right]g\left(\left|\mathbf{r}-\mathbf{r}'\right|\right)h(E), \qquad (19)$$

which confirms the KS deduction of short correlation distance $|\mathbf{r} - \mathbf{r}'|$, that led to the approximate self-energy form in Equation 12. Thus the energies can be well modeled by a simple functional form as a function of position.

Strong correlation in *d* and *f* electron materials

Materials containing active *d* and *f* electrons possess strong electron–electron correlations. Hubbard pointed out the origin as electron interaction within the same atom, providing the famous same-site interaction *U* for the much-used Hubbard model.[28,29] Since these electrons form narrow bands, LDA (including the spin extension) based on the homogeneous electron gas is inadequate. A possible route is to combine broadband computation using LDA with the narrow band by the hybridization model of Anderson[30] extending the single local impurity to a lattice. In References 31–33, we took into account the effect of the local interaction by a fluctuation of second order in *U*. The approximation was first tested in a one-dimension model against the exact numerical Monte Carlo computation. Then we applied the combined method to study the 3*d* magnetic elements where the *d* electrons are treated as localized states. The resultant quasiparticle energies with finite lifetimes provided an explanation for the origin of the spectral shape of photoelectron emissions and absorptions. By the same method, we found an explanation for the variation of the effective mass of "heavy fermions" in the uranium compound UX_3 with three elements of the platinum group, including iridium and gold. This result cannot be obtained by varying the parameters in the Hubbard model alone.

Test of the second-order U fluctuation in a 1D model

The test of the fluctuation of second order in *U* was carried out in a one-dimension model of a sinusoidal and half-filled *d*-band from the nearest neighbor hopping parameter, the *d–f* hybridization energy *V* and the *f–f* interaction *U*.[31]

For $U = 4$ and $V = 0.375$ in units of the noninteracting bandwidth, the poles of the Green's functions yield the quasiparticle energies and associated inverse lifetimes. There were four quasiparticle bands (spin-resolved). Two bands were close to the noninteracting bands with the *d–f* hybridization gap reduced drastically from the bare $2V$ value by the *f* state occupation. The highest and lowest states were the Hubbard states in bands.

The total energy driven by the U^2 fluctuation agreed with the accurate Monte Carlo results for $U = 0$ to 3. Moreover, the small *U* limit by perturbation and the large *U* limit by small *V/U* approximation were both checked to be correct. Thus, a smooth interpolation between the two limits is also possible.

Quasiparticle properties of Fe, Co, and Ni

This transition magnetic series is a good candidate for the computational method previously described.[32] The extended 4*s*, 4*p* orbitals form broad bands that can be covered by the LDA (including spin). The 3*d* atomic orbital has about 90% of its wave function inside the Wigner–Seitz spherical cell and thus can be modeled by the Hubbard onsite interaction and hybridization with the broad bands. The two-step procedure was the same as in the 1D model, with two changes: in the first step an *ab initio* computation of the band structure replaced the model one; and in the second step, the two-particle correlations were driven by the local interaction *U* and the additional exchange counterpart *J* involving all the *d* orbital and spin states in the same site. Each fluctuation computed was the difference between the two-particle correlation and the product of two mean expectation values from the first step. While the first-order terms in *U*, *J* can drive magnetism, the second-order terms change the 3*d* bandwidth and the effective electron mass and create additional features in the density of states and, therefore, the optical spectra. The calculated results showed that, while the ground-state properties such as partial occupation numbers and the Fermi surfaces from our inclusion of the *d* electron correlation effects were similar to the LDA method, the significantly better results were in the quasiparticle properties, such as the effective mass from the specific heat measurements and exchange splitting, and the quasiparticle lifetime for the features in x-ray photoelectron spectra, spin-resolved angle-resolved photoemission spectra, and the inverse process called bremsstrahlung isochromat spectra.[32]

Trend of heavy fermion occurrence in UX3, X = Ir, Pt, Au

The discovery in $CeAl_3$ of a very large electron effective mass from the specific heat in the linear low-temperature regime of the coefficient $\gamma = 1620$ mJ/mole K^2 spurred the finding of heavy fermions in numerous rare-earth intermetallic compounds and theories.[33,34] In Table I,[35–38] the local interaction was taken at $U = 2$ eV for uranium[39] for all three compounds being weakly dependent on the surroundings of a uranium atom.

The LDA results showed variation but no strong heavy mass effect. The inclusion of the correlation fluctuation showed a variation that matches the experimental data well. The contribution of the effective mass came from the electrons

Table I. Comparison of specific heat data with LDA and LDA plus local correlation results.

γ (mJ/K_2 per mole)	UIr_3	UPt_3	UAu_3*
Experiment	19.5	452	260
LDA	13.1	25.9	28.1
Plus local interaction	17	475	243
Experiment source	Ref. 36	Ref. 37	Ref. 38

*The actual structure was claimed by Reference 36 to be U14Au51.
Note: LDA, local density approximation.

https://doi.org/10.1557/mrs.2020.192 Published online by Cambridge University Press

near the Fermi level. The calculated results showed that the $j = 5/2$ peak covering the Fermi level was dominant over $j = 7/2$ about an eV above (j being the magnitude of the sum of the orbital angular momentum and spin). This determined the trend of the three compounds. It was also confirmed by the similar behavior in the pseudobinary alloys of UPd_3 and URh_3 from the evidence by the de Haas–van Alphen measurement[40] and the resonant photoelectron emission.[41]

Summary

While the paradigm of finding out the landscape by the human population distribution may seem outlandish, since the technology of shaping the landscape is here, the use of the population distribution is not a bad idea. The exchange of the roles between the potential and the density in the HK theorem may be viewed quite logically as the Legendre transformation. To demonstrate its power, I used the example of some quantum phase transitions (namely the phase transition at zero temperature) that make the Legendre transformation from the magnetic field at a spin site to the spin's magnetization to calculate the quantum entanglement as a signature for the phase transition.

By the quantum viewpoint of the density distribution as one slice of the tomography measurement of the system, we see the limitation of the HK theorem and the KS effort in changing a part of the kinetic energy back to the quantum form in terms of the momentum operator that does not commute with the position. KS equation is then a single-particle problem with all the electron interaction effects in the effective DFT potential.

The connection between the single electron without Coulomb interaction to the case with the interaction is expressed in terms of an infinite perturbation series. If the perturbation series is valid, then the effective potential is known and legitimate. A number of problems, such as the bandgap problem and good band structures, have in fact been solved.

In the strong electron interaction case, the theory is postulated to be beyond the perturbation theory. Some of us have made efforts to combination the KS band structure part with strong coupling fluctuations. They have yielded some interesting observations of the existence of the strongly correlated phenomena in some ferromagnets and heavy fermions but not others.

It would be interesting to see how much DFT can contribute to understanding the modern quantum materials.

Lu Jeu Sham is a Distinguished Professor Emeritus and a condensed-matter theorist at the University of California, San Diego. He received his BSc degree in mathematics from the Imperial College at the University of London, UK, and his PhD degree in theoretical condensed-matter physics from the University of Cambridge, UK. His research focuses on the many-body theory for first-principles computations of electron and phonon dynamics, including density functional theory; and also quantum optical processes in semiconductor nanostructures and spintronics, in collaboration with experimentalists. He is a member of the National Academy of Sciences and Academia Sinica, Republic of China, a Fellow of the American Physical Society, The Optical Society, and AAAS. Sham can be reached by email at ljsst@physics.ucsd.edu.

References

1. P. Hohenberg, W. Kohn, *Phys. Rev.* **136**, B864 (1964).
2. W. Kohn, L.J. Sham, *Phys. Rev.* **140**, A1133 (1965).
3. F. Herman, *Rev. Mod. Phys.* **30**, 102 (1958).
4. D. Bohm, D. Pines, *Phys. Rev.* **92**, 609 (1953).
5. M. Gell-Mann, K.A. Brueckner, *Phys. Rev.* **106**, 364 (1957).
6. J.B. Altepeter, E.R. Jeffrey, P.G. Kwiat, in *Advances in Atomic, Molecular, and Optical Physics*, P.R. Berman, C.C. Lin, Eds. (Elsevier, Amsterdam, The Netherlands, 2005), vol. 52, p. 105.
7. H.M. Wiseman, G.J. Milburn, *Quantum Measurement and Control* (Cambridge University Press, Cambridge, UK, 2010).
8. W. Kohn, L.J. Sham, *Phys. Rev.* **137**, A1697 (1965).
9. R.E. Langer, *Phys. Rev.* **51**, 669 (1937).
10. M. Thorpe, D. Thouless, *Nucl. Phys. A* **156**, 225 (1970).
11. J. Friedel, *Lond. Edinb. Dublin Philos. Mag.* **43**, 153 (1952).
12. L.-A. Wu, M.S. Sarandy, D.A. Lidar, L.J. Sham, *Phys. Rev. A* **74**, 052335 (2006).
13. S. Sachdev, *Quantum Phase Transitions* (Cambridge University Press, Cambridge, UK, 2001).
14. L.-A. Wu, M.S. Sarandy, D.A. Lidar, *Phys. Rev. Lett.* **93**, 250404 (2004).
15. W. Kohn, A.D. Becke, R.G. Parr, *J. Phys. Chem.* **100**, 12974 (1996).
16. L.J. Sham, W. Kohn, *Phys. Rev.* **145**, 561 (1966).
17. E. Wigner, *Phys. Rev.* **40**, 749 (1932).
18. L.J. Sham, *Phys. Rev. B* **32**, 3876 (1985).
19. J.M. Luttinger, J.C. Ward, *Phys. Rev.* **118**, 1417 (1960).
20. R.P. Feynman, *Phys. Rev.* **76**, 769 (1949).
21. J.P. Perdew, M. Levy, *Phys. Rev. Lett.* **51**, 1884 (1983).
22. L.J. Sham, M. Schlüter, *Phys. Rev. Lett.* **51**, 1888 (1983).
23. L.J. Sham, M. Schlüter, *Phys. Rev. B* **32**, 3883 (1985).
24. M. Lannoo, M. Schlüter, L.J. Sham, *Phys. Rev. B* **32**, 3890 (1985).
25. R.W. Godby, M. Schlüter, L.J. Sham, *Phys. Rev. Lett.* **56**, 2415 (1986).
26. R.W. Godby, M. Schlüter, L.J. Sham, *Phys. Rev. B* **35**, 4170 (1987).
27. R.W. Godby, M. Schlüter, L.J. Sham, *Phys. Rev. B* **36**, 6497 (1987).
28. J. Hubbard, *Proc. R. Soc. Lond. A Math. Phys. Sci.* **276**, 238 (1963).
29. J. Hubbard, *Proc. R. Soc Lond. A Math. Phys. Sci.* **277**, 237 (1964).
30. P.W. Anderson, *Phys. Rev.* **124**, 41 (1961).
31. M.M. Steiner, R.C. Albers, D.J. Scalapino, L.J. Sham, *Phys. Rev. B* **43**, 1637 (1991).
32. M.M. Steiner, R.C. Albers, L.J. Sham, *Phys. Rev. B* **45**, 13272 (1992).
33. M.M. Steiner, R.C. Albers, L.J. Sham, *Phys. Rev. Lett.* **72**, 2923 (1994).
34. K. Andres, J.E. Graebner, H.R. Ott, *Phys. Rev. Lett.* **35**, 1779 (1975).
35. A. Dommann, F. Hulliger, *J. Less-Common Met.* **141**, 261 (1988).
36. M.B. Brodsky, R.J. Trainor, A.J. Arko, H.V. Culbert, *AIP Conf. Proc.* **29**, 317 (1976).
37. G.R. Stewart, Z. Fisk, J.O. Willis, J.L. Smith, *Phys. Rev. Lett.* **52**, 679 (1984).
38. G.R. Stewart, *Rev. Mod. Phys.* **56**, 755 (1984).
39. J.F. Herbst, R.E. Watson, I. Lindgren, *Phys. Rev. B* **14**, 3265 (1976).
40. W. Ubachs, A. van Deursen, A. de Vroomen, A. Arko, *Solid State Commun.* **60**, 7 (1986).
41. B. Reihl, N. Mårtensson, D.E. Eastman, A.J. Arko, O. Vogt, *Phys. Rev. B* **26**, 1842 (1982). □

https://doi.org/10.1557/mrs.2020.192 Published online by Cambridge University Press